RSC Advances

ROYAL SOCIETY OF CHEMISTRY

www.rsc.org/advances

Cite this: DOI: 10.1039/c0xx00000x

www.rsc.org/xxxxxx

ARTICLE TYPE

Catalytic properties of Pd nanoparticles supported on Cu_2O microspheres for hydrogen peroxide electroreduction

Limei Sun*, Shuaishuai Zhang, Wuyunga Bao and Wurigamula He

Received (in XXX, XXX) Xth XXXXXXXXX 20XX, Accepted Xth XXXXXXXXX 20XX

DOI: 10.1039/b000000x

Abtract: Cuprous oxide(Cu_2O) were synthesized by a wet-chemical approach in aqueous solution and Pd electrocatalysts supported on cuporus oxide (Pd/ Cu_2O) and Vulcan XC-72 (Pd/C) were synthesized both via modified sodium borohydride reduction method. Scanning electron microscopy (SEM), X-ray diffraction (XRD), X-ray photoelectron spectroscopy (XPS) and cyclic voltammetry(CV) methods were used to characterize the surface morphology and composition of Cu_2O nanoparticles and the catalysts. Linear sweep voltammetry (LSV) and Chronoamperometry (CA) were employed to evaluate the activity and stability of the catalysts. The results showed that Cu_2O nanoparticles were spherical with smooth surface and the average diameter was about 600 nm. Pd nanoparticles decorated on the surface of Cu_2O nanospheres and agglomerated slightly and the average size of the Pd nanoparticles was about 10 nm. A certain amount of Copper oxide and the metallic Cu were formed during the preparation of the Pd/Cu_2O catalyst. The Pd catalyst supported on cuporus oxide (Pd/Cu_2O) shows the superior performance to the catalyst supported on Vulcan XC-72, which attributed to the two reasons. One was the Pd/Cu_2O catalyst had the larger surface area and the other was all of the support Cu_2O itself, Copper oxide and the metallic Cu formed in the process of catalyst preparation have activity to the H_2O_2 electroreduction reaction to a certain extent.

Keywords: Palladium; cuporus oxide; Hydrogen peroxide; Electroreduction reaction; Fuel cell..

1. Introduction

Fuel cells using hydrogen peroxide as oxidant, such as metal semi-fuel cells (MSFCs)[1-5], direct borohydride fuel cells (DBFCs)[6-9], with the merits of high energy density, capability of operating in an air-free environment (space and underwater), and easy storage and distribution of both the fuel and the oxidant[2, 10, 11], have grasped more attention recently.

The activity of electrocatalysts for H_2O_2 reduction influences directly the performance of the fuel cells using H_2O_2 as oxide, so the study on the catalysts of H_2O_2 electroreduction have been reported largely, which include: (1) noble metals, such as platinum, palladium, iridium, gold, silver and their alloy[1, 5, 11-16]; (2) macrocycle complexes of transition metals, such as Co porphyrin[17] and Cu triazine complexes[18, 19]; (3) transition metal oxides, such as cobalt oxides [10, 20, 21], uranium oxide[22], ferric oxides[23]. Among these catalysts, noble metal catalyst has the higher activity on the H_2O_2 reduction reaction, although meanwhile catalytic decomposition of hydrogen peroxide. Among them, noble metal Pd-based catalysts, such as Pd-Ir[24], Pd-Ag[12] and Pd-Ru[25], showed higher activity and better selectivity. These electrocatalysts are usually deposited on the support material to increase the surface area and reduce sintering effects. Carbon is a common choice for supporting nanosized electrocatalyst particles in low temperature fuel cells[14]. However, carbon materials only serve to support the noble metal nanoparticles but not to improve the activity of the composite catalyst. Therefore, more attention has been paid to the preparation of the composites between noble metals and other catalytic materials. A few studies using oxide material as active or promoting support have been reported in this regard. Examples are Pt/CuO[26], Pd/Co_3O_4[27] which can further enhance the performance of catalyst and also improve the efficiency of noble metals.

Both the oxide of copper, including of CuO[13, 28] and Cu_2O[29], have showed certain activity for H_2O_2 reduction action, however, they have low electric conductivity and catalytic performance. Many reports[26, 30-32] have revealed that these oxides decorated with metal particles could increase the conductivity and further improve the performance. In this study, we prepared Cu_2O nanopowders and Pd nanoparticles supported on cuprous oxide and investigated the promotion of the support for the performance of Pd-based catalysts on hydrogen peroxide electroreduction.

2. Experimental procedure

2.1. Reagents

Copper sulfate ($CuSO_4 \cdot 5H_2O$), glucose monohydrate ($C_6H_{12}O_6$), anhydrous ethanol (C_2H_5OH), were purchased from Tianjin

Kemiou Chemical Reagent Co. Ltd and $PdCl_2$, $NaBH_4$, NaOH, H_2SO_4, and H_2O_2 (30 wt.%) were supplied by Tianjin Tianda Chemical Preparation Co. Ltd. Vulcan XC-72(C) was obtained from Cabot Corp. with a specific surface area (BET) of 254 $m^2 g^{-1}$. Nafion solution (5 wt. %) was purchased from DuPont Corp. All chemicals were analytical grade and were used as-received without further purification. Ultrapure water (Millipore, 18 MΩ cm) was used throughout the study. separate the symbol from the text.

2.2. Catalyst preparation

The preparation of Cu_2O nanoparticles was carried out as follows. 0.2 mol CuSO4 was dissolved in 200 mL deionized water. Then 200 mL 2 mol L-1 NaOH aqueous solution was added dropwise with a speed of 2 mL min-1 to the above $CuSO_4$ solution under constant stirring. A blue precipitate of $Cu(OH)_2$ was produced, and 200 mL 2.5 mol L-1 glucose solution was added to the above suspension, and stirred constantly at 80 °C for 1 h. Then the brick red precipitates were produced and centrifugated, rinsed five times by using deionized water and rinsed two times by using anhydrous ethanol, then dried in a vacuous desiccator at 65 °C for 24 h.

The Pd/Cu_2O catalysts with Pd metal loading of 20 wt. % were obtained by the chemical reduction method. First, the pH of H_2PdCl_4 solution was adjusted to 8-9 by the NaOH solution. And then 60 mg Cu_2O nanopowders were added into the mixture and treated in an ultrasonic bath. 15 mL 1 mol L-1 NaBH4 solution was added drop by drop and stirred for 4 h. Finally, the mixtures were filtered, washed and dried under vacuum. To compare the characteristics of electrocatalysts, 20 wt. % Pd/C catalysts were prepared through the same procedure using Vulcan XC-72 as the support material.

2.3. Characterization

The crystal phase of the synthesized nanoparticles and the catalysts were identified by X-ray diffraction (XRD,D8FOCUS) using CuKα radiation (2 kV rotating anode, λ= 0.154056 nm). The samples were scanned from 20° to 90° at a scanning rate of 0.02° s-1. The microstructures and morphologies of the Pd/Cu_2O catalysts were determined by scanning electron microscopy (SEM,JSM-6480) and transmission electron microscope(TEM, H-7650). X ray photoelectron spectroscopy (XPS) measurements were carried out on a Thermo ESCALAB 250 with Al Kα radiation for the X-ray sources and the binding energy was calibrated by means of the C1s peak energy of 284.8 eV. The curves were fitted by using the XPSPEAK41 software.

2.4. Electrochemical characterizations

Electrochemical experiments were measured in a conventional three-electrode electrochemical cell using a glassy-carbon electrode (d = 5 mm) as the working electrode, Carbon rod as the auxiliary electrode, and a saturated calomel electrode (SCE) as the reference electrode. The coating of catalyst on glassy-carbon electrode was carried out as follows: the glassy-carbon electrode was polished with alumina power down to 0.3 μm, washed with ultrapure water and dried in air completely. 5 mg of the catalyst was mixed with 2 mL ultrapure water. The mixture was homogenized in an ultrasonic bath for 30 min to obtain catalyst suspension. 15 μL of the catalyst suspension was spread on the surface of the glassy carbon electrode with a loading of approximately 200 μg cm^{-2} and dried in air at room temperature for 2 h. Then, 5 μL of Nafion solution was applied to the glassy-carbon electrode and dried in air in order to prevent the catalyst from falling apart. Thus a thin layer of catalyst was fixed on the surface of glassy-carbon electrode.

Electrochemical measurements were performed on a PARSTAT 2273 Potentiostats-Electrochemistry Workstation (Ametek Corp.).Cyclic voltammetry measurements (CV) were conducted in the potential between -0.3 V and 1.2 V in 0.1 mol L^{-1} H_2SO_4 solution. Linear scan voltammetry (LSV) was obtained in 0.1 mol L^{-1} H_2SO_4 solution contain H_2O_2 with various concentration. The scan rates of the above two procedures were both 50 mV s^{-1} and the procedures were both repeated 5 times to obtain the stable results. Chronoamperometry (CA) was performed in 0.1 mol L^{-1} H_2SO_4 + 0.5 mol L^{-1} H_2O_2 solution for 1800 s at 0 V. The electrolyte solutions were saturated by bubbling high purity nitrogen for 20 min before the measurements and were protected with the nitrogen during potential cycling. All potentials in this paper are reported versus the saturated calomel electrode (SCE).

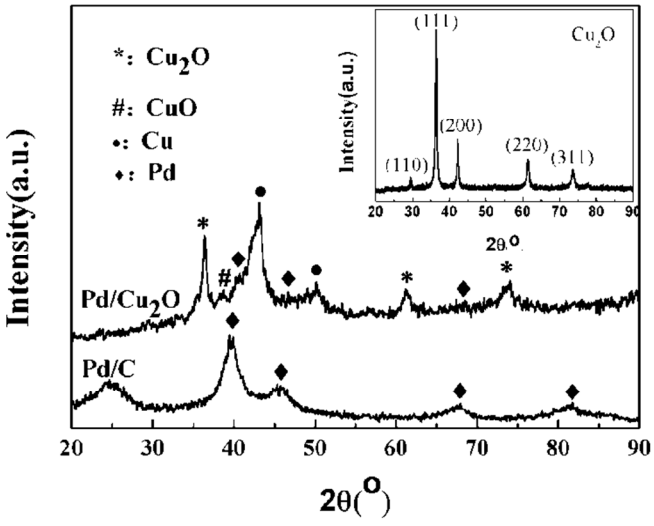

Fig.1 XRD pattern of Pd/Cu_2O and Pd/C samples. The inset shows XRD pattern of Cu_2O nanopowders.

Cite this: DOI: 10.1039/c0xx00000x

www.rsc.org/xxxxxx

ARTICLE TYPE

3. Results and discussion

3.1. Catalyst characterization

XRD measurements were carried out to obtain the structural information for the prepared Cu_2O nanopowders and the two catalysts obtained from different catalyst carriers. Figure 1 shows the XRD patterns of the Pd/Cu_2O and Pd/C catalysts, and the insert shows the XRD patterns of the Cu_2O nanopowders. From the insert, peaks were observed at about 2θ = 29.8º, 36.7º, 42.5º, 61.5º and 73.7º, which were characteristic of cubic Cu_2O phase(JCPDS Card No. 65-3288). From the pattern of the Pd/C catalyst, the diffraction peaks at about 39.9º, 46.4º, 67.8º and 81.6º are attributed to the Pd (111), Pd (200), Pd (220) and Pd (311) planes of face-centered cubic (fcc) phase(JCPDS Card No. 65-2867) and the peak at about 25º was associated with the Vulcan XC-72 support material. From the pattern of the Pd/Cu_2O catalyst, besides the cubic Cu_2O phase and the Pd fcc phase, some unexpectedly characteristic peaks are observed. The peak at 38.8 º is attributed to the CuO(111) planes(JCPDS Card No. 65-2309) and the peaks at 43.3 º and 50.4 º can be indexed to (111) and (200) planes of the Cu crystal structure (JCPDS Card No. 04-0836).The results demonstrate that some Cu^+ ions have been oxidized to the Cu2+ ions and at the same time, others have been reduced to the metallic Cu by $NaBH_4$ during the preparation of the Pd/Cu_2O catalyst.

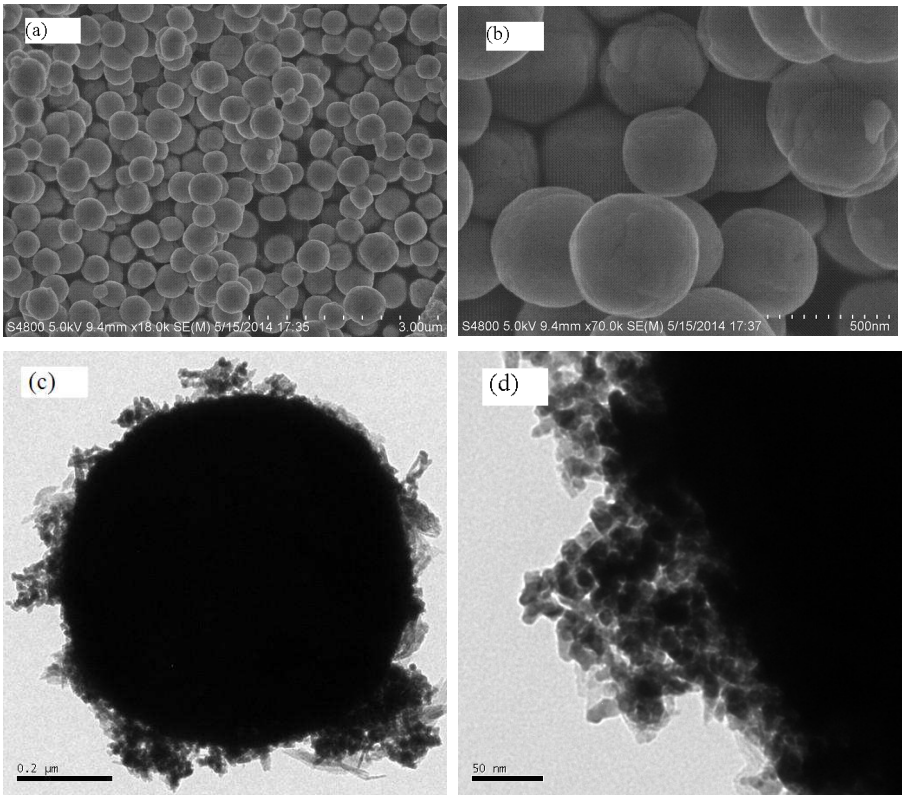

Fig.2 (a), (b) SEM images of Cu2O nanopowders. (c), (d) TEM images of Pd/Cu2O catalysts.

Figure 2(a) and (b) shows the SEM images of the Cu2O samples in different resolutions, respectively. It can be seen that the Cu2O particles prepared are in a spherical shape with smooth surface as well as high dispersity and the average diameter of the spheres is about 600 nm. Fig.2(c) shows the TEM image of the Pd/Cu2O catalyst and fig. 2(d) is the corresponding high magnification images. Pd nanoparticles decorate on the surface of Cu2O nanospheres and agglomerate slightly together to form larger clusters and the average size of the Pd nanoparticles is about 10 nm. It was confirmed from the SEM and TEM that Pd/Cu2O composite microspheres with core-shell structure were obtained.

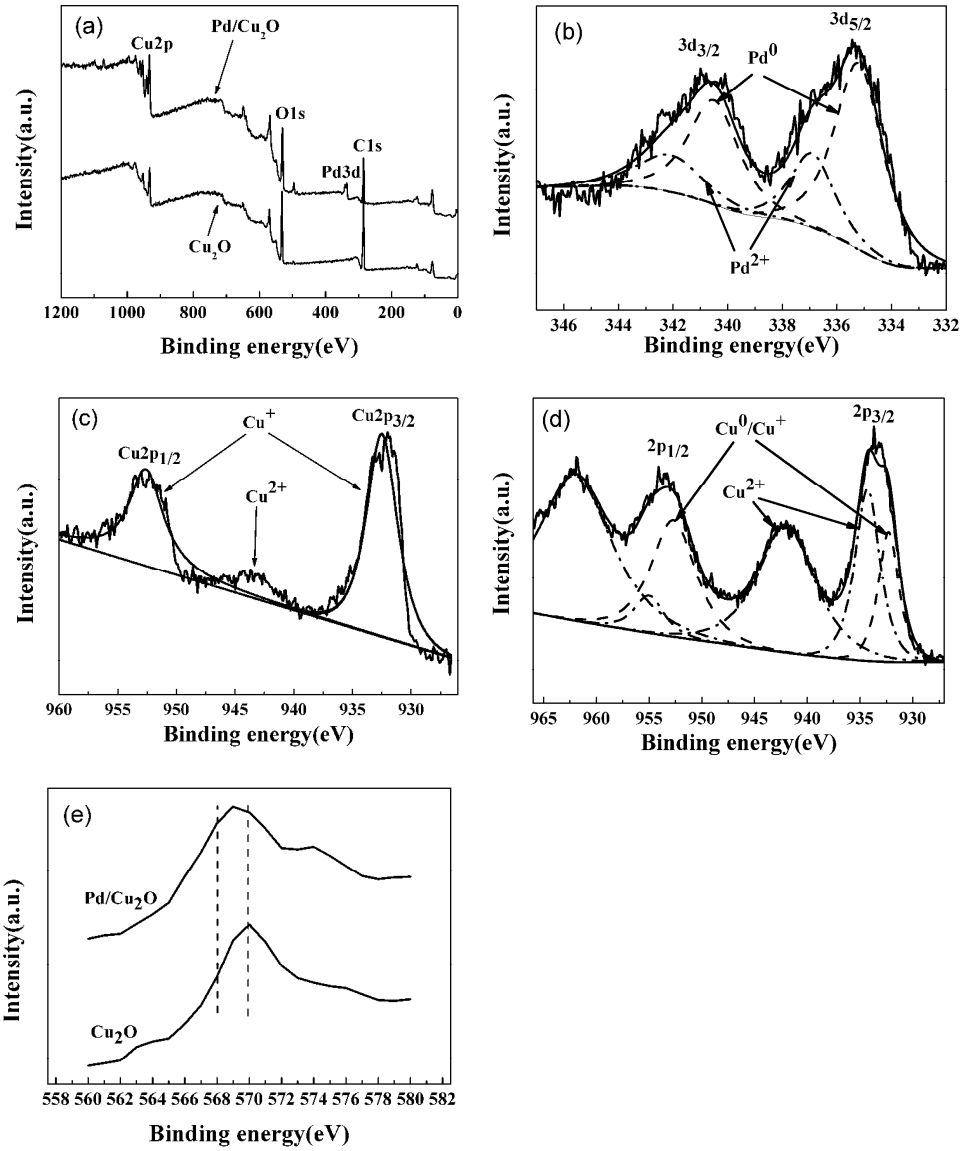

Fig.3 (a) XPS survey spectra of Cu_2O and Pd/Cu_2O samples. (b) Pd3d scan spectra of Pd/Cu_2O samples. (c) (d) Cu2p scan spectra of Cu_2O and Pd/Cu_2O samples. (e) Cu LMM-2 auger transition of Cu_2O and Pd/Cu_2O samples.

X-ray photoelectron spectroscopy (XPS) was used to determine the surface composition and possible electronic interactions of the Cu_2O nanopowders and the Pd/Cu_2O catalysts. A typical survey XPS spectrum in Fig. 3(a) reveals that both samples are composed of Cu and O elements, while an additional peak assigned to Pd element appears in XPS spectrum of Pd/Cu_2O, which indicates the presence of Pd species on Cu_2O. Fig. 3(b) presents the high resolution XPS scan spectra of Pd3d. As shown in Fig. 3(b), the Pd 3d signal of the Pd/Cu_2O catalyst can be fitted to two pairs of doubles: Pd 3d3/2 (340.5 eV), Pd 3d5/2 (335.2 eV) and Pd 3d3/2 (342.2 eV), Pd 3d5/2 (337.0 eV), which can be assigned to Pd0 and PdIIO species, respectively[33]. Fig. 3(c) and (d) show the Cu 2p XPS scan spectra of Cu_2O and Pd/Cu_2O samples, respectively. The fitting Cu2p spectrum (Fig. 3(c)) shows the peaks at 932.5 eV and 952.5 eV, which were corresponding to the Cu 2p3/2 and Cu 2p1/2 of the Cu_2O[34],respectively. As shown in Fig. 3(d), the peak fit of the Cu 2p3/2 core level for the Pd/Cu_2O catalyst revealed two binding energy states at 932.0 and 942.0 eV, which were assigned to Cu_2O and CuO [33, 35]. Moreover, a satellite signal at 934.4 eV was also assigned to CuO [36], It is obvious that a considerable amount of CuO exists on the surface of the Pd/Cu_2O catalyst, supporting the presence of the characteristic peak of CuO (1 1 1) in the XRD pattern of the Pd/Cu_2O catalyst. Although some Cu^0 should also exist on the catalyst surface, it is hard to be discriminated from Cu_2O due to their similar binding energy. One can distinguish them from the position of their LMM-2 auger transition in XPS spectra which are about 568 eV and 570 eV for Cu and Cu_2O, respectively[37] . From Fig.3(e), it can be seen that there is a peak at about 570 eV in the XPS spectra of Cu_2O samples, thus it can be make a certain conclusion that the 932.0 eV in Fig.3(c) is related to Cu_2O. However, the peak at 569 eV in the XPS spectra of Pd/Cu_2O samples revealed two binding energy states at 968.0 and

970.0 eV, which are attributed to Cu^0 and Cu+ ions ,respectively. This illustrates a certain quantity of the metallic Cu also exists on the surface of the Pd/Cu_2O catalyst which is in agreement with that discussed in XRD.

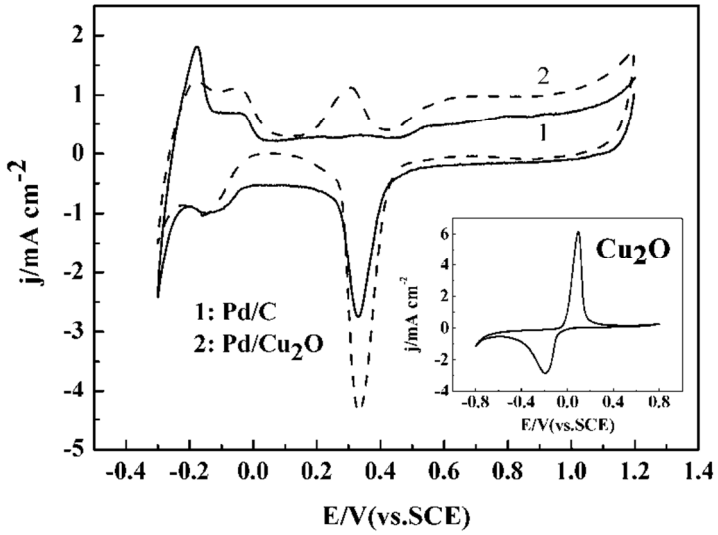

Fig.4 Cyclic voltammograms of Pd/C and Pd/Cu_2O catalysts in 0.1 mol/L H_2SO_4 solution at a scan rate of 50 mV/s.

3.2. Electrochemical measurements

Figure 4 shows cyclic voltammograms(CV) of the Pd/Cu_2O and Pd/C catalysts in 0.1 mol/L H_2SO_4 solution, and the insert is the CV of Cu_2O nanopowder. It can be seen from the insert, a pair of nearly reversible redox peaks were observed at about -0.2 V and 0.1 V (versus SCE) which can be attributed to the reduction of CuO/Cu2O redox couple[29]. The shape of the voltammeter curve of the Pd/Cu_2O and Pd/C catalysts is very similar and both samples exhibit a hydrogen adsorption / desorption peak at –0.3 V – 0 V and Pd-oxide formation/reduction peak at 0.5 V–1.2 V. The reduction of palladium oxide of the Pd/Cu_2O or Pd/C catalyst shows a well-defined cathodic peak between 0.1 V and 0.5 V. However, the anodic peak at 0.3 V in the Pd/Cu_2O catalyst, which was not seen in the Pd/C sample, indicates the oxidation of an Cu–O species[33].It is due to a certain quantity of the metallic Cu exists on the surface of the Pd/Cu_2O catalyst, which is consistent with the findings in XRD and XPS. The electrochemically active surface area (EASA) of the catalysts can be calculated from the charge obtained from the cathodic peak between 0.1 V and 0.5 V. Pd assumes that a monolayer of PdO was formed and its reduction charge value is 405 $\mu C/cm^2$ [38]. Such estimated EASA of the Pd/Cu_2O and Pd/C catalysts are 53.3 m^2/g_{Pd} and 30 m^2/g_{Pd}, respectively. This indicated that the Pd/Cu_2O electrode has the larger surface area than the Pd/C electrode.

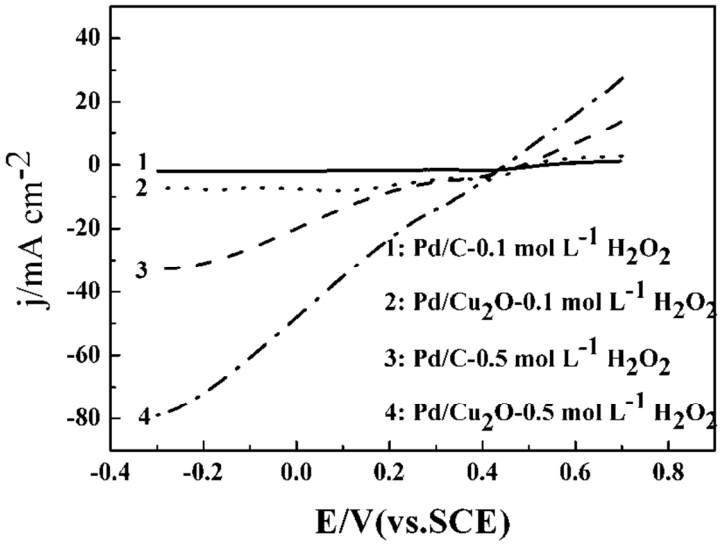

Fig.5 Linear sweep voltammograms of Pd/C and Pd/Cu_2O catalysts in 0.1 mol/L H_2SO_4 solution with different concentration at a scan rate of 50 mV/s.

Figure 5 shows linear sweep voltammograms of the Pd/Cu_2O and Pd/C catalysts in N_2-saturated 0.1 mol L^{-1} H_2SO_4 solutions with various H_2O_2 concentrations at a scan rate of 50 mV s^{-1}. It can be seen that both the current density for hydrogen peroxide electroreduction on the two catalysts increase with the concentration of H_2O_2 increasing and the current density on Pd/Cu_2O electrode has been higher than that on the Pd/C electrode, which indicate that the catalytic activity of the Pd/Cu_2O electrode is higher than that of the Pd/C. There are two reasons leading to the higher catalytic activity of the Pd/Cu_2O catalyst. One is the Pd/Cu_2O electrode has a larger specific surface and the other may be that both the support Cu_2O itself[29] and two other products formed during the preparation of the Pd/Cu_2O catalyst, including CuO[13, 28] and the metal Cu[39] , show certain activity for the action of H_2O_2 reduction except the noble metal Pd has the higher catalytic activity on H_2O_2 reduction in acid medium[11]. There have been several studies of the electroreduction action of hydrogen peroxide on the Cu and its oxides surface in different pH solution[13, 18, 39, 40]. It has been shown that the catalysis in this action is brought about by the Cu(II)/Cu(I) and Cu(I)/Cu(0) couples. As shown in Equation (1)-(4), Cu with the higher valence in the couples, such as Cu(II) and Cu(I), firstly reduced electrochemically to Cu with the low valence, such as Cu(I) and Cu(0) , which reacted chemically with H_2O_2 and resulted in the H_2O_2 revert to OH^- and in the regeneration of the catalyst.

$$2CuO+H_2O+2e \rightarrow Cu_2O+2OH^- \quad (1)$$ or

$$Cu_2O+H_2O+2e \rightarrow 2Cu+2OH^- \quad (2)$$

$$Cu_2O+H_2O_2 \rightarrow 2CuO+H_2O \quad (3)$$ or

$$2Cu+H_2O_2 \rightarrow Cu_2O+H_2O \quad (4)$$

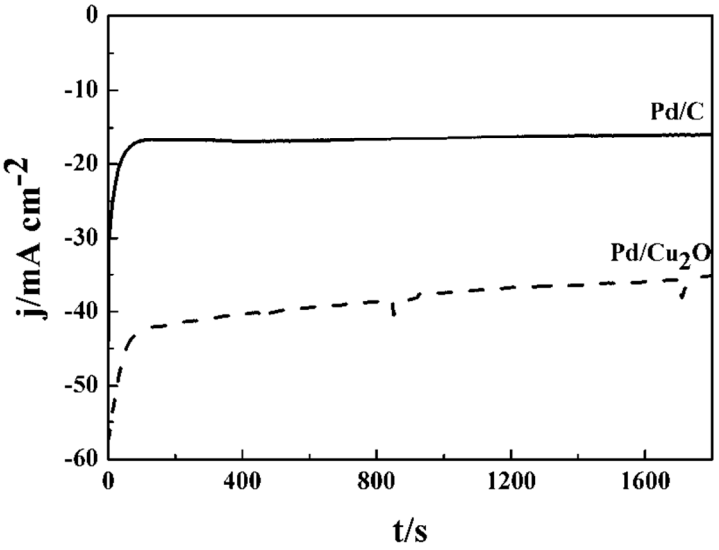

Fig.6 chronoamperometry of Pd/C and Pd/Cu_2O catalysts in 0.1 mol/L H_2SO_4 +0.5 mol/L H_2O_2 solution at a scan rate of 50 mV/s.

Chronoamperometry tests for hydrogen peroxide electroreduction reaction on the Pd/Cu_2O and Pd/C catalysts were performed at 0 V for 1800 s. As is shown in Fig. 6, two catalysts exhibit excellent stability although the current density on the two catalysts slightly decreases during the test because of the depletion of H_2O_2 near the electrode surface. The current density for hydrogen peroxide electroreduction reaction of Pd/Cu_2O catalyst (about 38 mA cm^{-2}) is higher than that of Pd/C (about 17 mA cm^{-2}). This agrees well with the study of linear sweep voltammetry. The higher current density can be attributed to the higher active surface area and the promoting effect of the supports to the Pd catalyst for the hydrogen peroxide electroreduction reaction.

4. Conclusions

In this work, cuprous oxide nanoparticles were synthesized by a wet-chemical approach in aqueous solution and the Pd catalysts supported on Cu_2O and C were prepared by means of a modified sodium borohydride reduction method. As a result, the Cu_2O nanosphere was cubical shape and the size was about 600 nm. The palladium decorated on Cu_2O as metal with face-centered cubic structure and the particle size was about 10 nm. The metallic Cu and CuO produced during the synthesis of the Pd/Cu_2O composites. The reduction reaction of Hydrogen peroxide on the Pd/Cu_2O catalyst has good stability and higher current density. This was due to that (1) the Pd/Cu_2O catalyst has the larger surface area; (2) the support Cu_2O and the metallic Cu and CuO produced in preparation process improved the activity of Pd towards H_2O_2 reduction reaction. Using this method, catalysts are prepared in aqueous solution easily with high catalytic activity and lower cost, which has great potential in industrial application.

This work was financially supported by the National Natural Science Foundation of China (21003070; 21463017) and the Natural Science Foundation of Inner Mongolia, China (2012MS0208).

Notes and references

a College of Chemistry and Chemical Engineering，Inner Mongolia University for the Nationalities，TongLiao，China；E-mail：sunlimei2000@163.com

1. R. R. Bessette, J. M. Cichon, D. W. Dischert and E. G. Dow, *Journal of Power Sources*, 1999, **80**, 248-253.
2. Ø. Hasvold, K. H. Johansen, O. Mollestad, S. Forseth and N. Størkersen, *Journal of Power Sources*, 1999, **80**, 254-260.
3. L. An, T. S. Zhao, X. L. Zhou, X. H. Yan and C. Y. Jung, *Journal of Power Sources*, 2015, **275**, 831-834.
4. M. G. Medeiros, R. R. Bessette, C. M. Deschenes and D. W. Atwater, *Journal of Power Sources*, 2001, **96**, 236-239.
5. M. G. Medeiros, R. R. Bessette, C. M. Deschenes, C. J. Patrissi, L. G. Carreiro, S. P. Tucker and D. W. Atwater, *Journal of Power Sources*, 2004, **136**, 226-231.
6. D. Cao, Y. Gao, G. Wang, R. Miao and Y. Liu, *International Journal of Hydrogen Energy*, 2010, **35**, 807-813.
7. N. A. Choudhury, R. K. Raman, S. Sampath and A. K. Shukla, *Journal of Power Sources*, 2005, **143**, 1-8.
8. T. H. Oh, B. Jang and S. Kwon, *Energy*, 2014, **76**, 911-919.
9. L. Yi, L. Liu, X. Wang, X. Liu, W. Yi and X. Wang, *Journal of Power Sources*, 2013, **224**, 6-12.
10. D. Cao, J. Chao, L. Sun and G. Wang, *Journal of Power Sources*, 2008, **179**, 87-91.
11. D. Cao, L. Sun, G. Wang, Y. Lv and M. Zhang, *Journal of Electroanalytical Chemistry*, 2008, **621**, 31-37.
12. W. Yang, S. Yang, W. Sun, G. Sun and Q. Xin, *Electrochimica Acta*, 2006, **52**, 9-14.
13. X. M. Miao, R. Yuan, Y.-Q. Chai, Y.-T. Shi and Y.-Y. Yuan, *Journal of Electroanalytical Chemistry*, 2008, **612**, 157-163.
14. L. Sun, Z. Liu, Y. Bao, H. Li and W. Bao, *International Journal of Materials Research*, 2014, **105**, 584-587.
15. X. Jing, D. Cao, Y. Liu, G. Wang, J. Yin, Q. Wen and Y. Gao, *Journal of Electroanalytical Chemistry*, 2011, **658**, 46-51.
16. A. L. Morais, J. R. C. Salgado, B. Šljukić, D. M. F. Santos and C. A. C. Sequeira, *International Journal of Hydrogen Energy*, 2012, **37**, 14143-14151.
17. H. Liu, L. Zhang, J. Zhang, D. Ghosh, J. Jung, B. W. Downing and E. Whittemore, *Journal of Power Sources*, 2006, **161**, 743-752.
18. M. V. Vazquez, S. R. de Sanchez, E. J. Calvo and D. J. Schiffrin, *Journal of Electroanalytical Chemistry*, 1994, **374**, 179-187.
19. D. Deletioğlu, S. Yalçınkaya, C. Demetgül, M. Timur and S. Serin, *Materials Chemistry and Physics*, 2011, **128**, 500-506.
20. K. Cheng, D. Cao, F. Yang, Y. Xu, G. Sun, K. Ye, J. Yin and G. Wang, *Journal of Power Sources*, 2014, **253**, 214-223.
21. X. Xiao, F. Yang, K. Cheng, X. Wang, J. Yin, K. Ye, G. Wang and D. Cao, *Journal of Electroanalytical Chemistry*, 2014, **729**, 103-108.
22. J. S. Goldik, J. J. Noël and D. W. Shoesmith, *Journal of Electroanalytical Chemistry*, 2005, **582**, 241-248.
23. L. Zhang, Y. Ni, X. Wang and G. Zhao, *Talanta*, 2010, **82**, 196-201.
24. R. R. Bessette, M. G. Medeiros, C. J. Patrissi, C. M. Deschenes and C. N. LaFratta, *Journal of Power Sources*, 2001, **96**, 240-244.
25. L. Sun, D. Cao and G. Wang, *J Appl Electrochem*, 2008, **38**, 1415-1419.
26. R. S. Amin, R. M. Abdel Hameed, K. M. El-Khatib, H. El-Abd and E. R. Souaya, *International Journal of Hydrogen Energy*, 2012, **37**, 18870-18881.
27. K. Cheng, F. Yang, Y. Xu, L. Cheng, Y. Bao, D. Cao and G. Wang, *Journal of Power Sources*, 2013, **240**, 442-447.
28. Y. Li, D. Cao, Y. Liu, R. Liu, F. Yang, J. Yin and G. Wang, *International Journal of Hydrogen Energy*, 2012, **37**, 13611-13615.
29. L. SUN and J. CHEN, *International Journal of Nanoscience*, 2012, **11**, 1240027-1240030.
30. X. Guo, P. Diao, D. Xu, S. Huang, Y. Yang, T. Jin, Q. Wu, M. Xiang and M. Zhang, *International Journal of Hydrogen Energy*, 2014, **39**, 7686-7696.
31. J. Ma, S. Guo, X. Guo and H. Ge, *Surface and Coatings Technology*, 2015.
32. S. Wei, J. Shi, H. Ren, J. Li and Z. Shao, *Journal of Molecular Catalysis A: Chemical*, 2013, **378**, 109-114.
33. L. Lu, L. Shen, Y. Shi, T. Chen, G. Jiang, C. Ge, Y. Tang, Y. Chen and T. Lu, *Electrochimica Acta*, 2012, **85**, 187-194.
34. W. Xu, S. Zhu, Z. Li, Z. Cui and X. Yang, *Electrochimica Acta*, 2013, **114**, 35-41.
35. C. Xu, Y. Liu, J. Wang, H. Geng and H. Qiu, *Journal of Power Sources*, 2012, **199**, 124-131.
36. B. Zeng, X. Chen, X. Ning, C. Chen, A. Hu and W. Deng, *Catalysis Communications*, 2014, **43**, 235-239.
37. S. Min, F. Wang, Z. Jin and J. Xu, *Superlattices and Microstructures*, 2014, **74**, 294-307.
38. T. Chierchie, C. Mayer and W. J. Lorenz, *Journal of Electroanalytical Chemistry and Interfacial Electrochemistry*, 1982, **135**, 211-220.
39. K. L. Stewart and A. A. Gewirth, *Langmuir*, 2007, **23**, 9911-9918.
40. S. Ceré, M. Vazquez, S. R. de Sánchez and D. J. Schiffrin, *Journal of Electroanalytical Chemistry*, 1999, **470**, 31-38.